

# Effect of Holding Time on Optical Structure Properties of Ba(Zr<sub>0.5</sub>Ti<sub>0.5</sub>)O<sub>3</sub> Thin Film Using Sol-Gel Method

Taufiq Hidayat, Rahmi Dewi\*, Yanuar Hamzah  
Department of Physics, Universitas Riau, Pekanbaru, Indonesia

## ABSTRACT

The ferroelectric thin film material of barium zirconium titanate (BZT) on the fluorine-doped tin oxide (FTO) glass substrate was successfully prepared using the sol-gel method. The purpose of this study was to determine the effect of crystal size on the variation of holding time. The lattice parameter data has a value of  $a = b$  of 3.918 Å and for  $c$  it is 4.01 Å. The results of this study indicate that the crystal structure of BZT is tetragonal because the lattice parameter has the same values  $a$  and  $b$  but not equal to  $c$ . To obtain the bandgap energy, a thin film plot method of Ba(Zr<sub>0.5</sub>Ti<sub>0.5</sub>)O<sub>3</sub> was used at a temperature of 700 °C with a holding time of 30 minutes, 1 hour, 1 hour 30 minutes, and 2 hours. The optical thin layer bandgap energy of Ba(Zr<sub>0.5</sub>Ti<sub>0.5</sub>)O<sub>3</sub> was calculated using the Tauc plot. The absorbance values obtained were 3.277 a.u., 3.0654 a.u., 3.323 a.u., and 3.424 a.u. The maximum transmission (TM) occurs at 1 hour holding time which gives a percentage of TM<sub>1</sub> 44.477% and TM<sub>2</sub> 20.568%. While the 2 hour hold time gives a minimum transmission (Tm) of Tm<sub>1</sub> 10.859% and Tm<sub>2</sub> 7.759%, respectively.

## ARTICLE INFO

### Article history:

Received Oct 16, 2020

Revised Nov 3, 2020

Accepted Dec 24, 2020

### Keywords:

Thin film BZT  
Holding time  
Crystal structure  
Energy gap

This is an open access article under the [CC BY](#) license.



### \* Corresponding Author

E-mail address: drahmiz002@yahoo.com

## 1. INTRODUCTION

Barium Titanate (BaTiO<sub>3</sub>) is a ferroelectric material that is often used for applications in the electronics field [1]. BaTiO<sub>3</sub> is a ferroelectric oxide material with a perovskite ABO<sub>3</sub> [2] structure which is widely used for charge storage due to its characteristic variations [3]. The Curie temperature at BT is 130 °C [4]. To increase the dielectric constant [5,6] and to reduce dielectric losses at low frequencies [7], Strontium (Sr) or zirconium (Zr) is added.

Barium zirconium titanate (BZT) is a material that replaces BST because Zr<sup>4+</sup> has more stable chemical properties than Ti<sup>4+</sup>, has a larger ion size and to expand the perovskite lattice. In addition, the radius of Zr<sup>4+</sup> is 0.087 nm, which is greater than the radius of Ti<sup>4+</sup>, which is 0.068 nm [8]. The BZT thin layer has a fine grain structure [9] and dense has good dielectric properties [10]. BZT material has a high dielectric constant [11], low dielectric loss [12], low leakage current density [13]. A high dielectric constant will increase the capacitance of a higher charge [14,15] so that the load storage is more [16].

Several methods that can be used in the growth of thin films include: sol-gel process [17,18], sputtering [19,20], Hydrothermal [21], Chemical Solution Deposition (CSD) [22], Solid State Reaction [23,24], Metal Organic Chemical Vapor Deposition (MOCVD) [25], Pulsed Laser Deposition (PLD) [8,26]. In this study, a thin layer of Barium Zirconium Titanate was grown with the composition Ba(Zr<sub>0.5</sub>Ti<sub>0.5</sub>)O<sub>3</sub> using the sol-gel method. This research was conducted with annealing process at 700 °C with variation of holding time 30 minutes, 1 hour, 1 hour 30 minutes and 2 hours in order to get a good level of homogeneity and a better level of crystallinity. Furthermore, the characterization test will be carried out including using X-Ray Diffraction (XRD) equipment, Ultraviolet Visible (UV-Vis) Spectroscopy.

## 2. RESEARCH METHODS

$Ba(Zr_xTi_{1-x})O_3$  solution grown on the surface of the substrate using the Sol-gel method was prepared by reacting barium acetate, zirconium dioxide, titanium isopropoxide and solvents for acetyl acid, acetyl acetone and ethylene glycol. Mixing  $BaCO_3$ ,  $ZrO_2$  with 8 ml acetyl acid solvent and 2 ml aqua DM and  $Ti(OC_3H_7)_4$  with 0.5 ml ethylene glycol and 16 ml ethanol in sample  $x = 0.5$  then the sample is put into a bottle that has been done sonication stage like the schematic above. Then stirring in each solution with a magnetic stirrer on a hot plate with a speed of 250 rpm and a temperature of  $31.6^\circ C$ . Then after the  $BaCO_3$  solution is clear,  $ZrO_2$  and  $Ti(OC_3H_7)_4$  clear the solution is mixed with  $Zr + Ti$ . After the two solutions are mixed, wait until they clear, then mix with  $BaCO_3$  so that it will become a  $Ba + Zr + Ti$  solution then mix 4 drops of acetyl acetone ( $C_5H_8O_2$ ) for several hours then it will become BZT solvent.

$Ba(Zr_xTi_{1-x})O_3$  solution where  $x = 5$  which has become BZT solvent is then followed by a spin coating process for 30 seconds at a speed of 3600 rpm. Then the substrate was heated to the initial pre annealing temperature in an oven at  $150^\circ C$  for 30 minutes then heated again at  $300^\circ C$  to remove various objects such as  $O_2$  and  $CO_2$  in the sample. After that, it was annealed with a furnace at  $700^\circ C$  with a holding time of 30 minutes, 1 hour, 1 hour 30 minutes and 2 hours.

## 3. RESULTS AND DISCUSSION

### 3.1. Structure and Lattice Diffraction

Characterization using XRD BZT grown on an Fluorine Tin Oxide (FTO) substrate with the composition  $Ba(Zr_{0.5}Ti_{0.5})O_3$  shows the measurement results related to the intensity of the diffraction peak (representing the y axis) with an angle of  $2\theta$  (representing the x axis). The crystal structure can be determined by looking at the position of the peaks listed in the graph of the relationship  $2\theta$  with the intensity of the diffraction peaks.

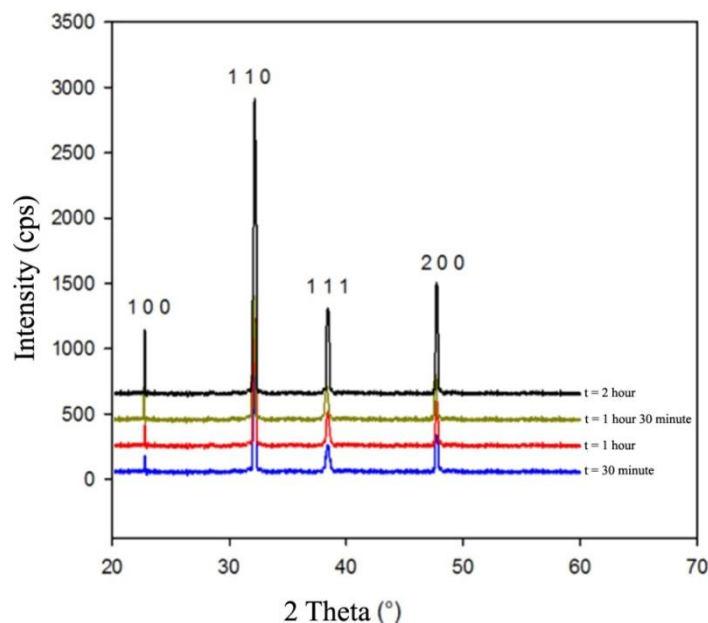


**Figure 1.** XRD diffraction pattern of  $Ba(Zr_{0.5}Ti_{0.5})O_3$  thin layer at  $700^\circ C$  holding time of 30 minutes, 1 hour, 1 hour 30 minutes and 2 hours.

Figure 1 shows the diffraction pattern of the BZT thin film with a holding time variation at  $700^\circ C$ .  $d_{hkl}$  data and identified peaks belong to BZT holding time of 30 minutes, 1 hour, 1 hour 30 minutes and 2 hours. Table 1 is the result of data processing of  $Ba(Zr_{0.5}Ti_{0.5})O_3$  thin layer at  $700^\circ C$ . Table 1 shows that the peaks found on the graph represent the plane orientation which is assumed to belong to  $Ba(Zr_{0.5}Ti_{0.5})O_3$  with the same plane. At a temperature of  $700^\circ C$  a holding time of 1 hour 30 minutes with  $(2\theta)$  plane  $(2\ 0\ 0)$  with an angle of  $47.73^\circ$  with an intensity of 427.1 cps produces the highest intensity peak, the addition of holding time will affect the diffraction angle and intensity. The Sintechem, 1(2), 59-66

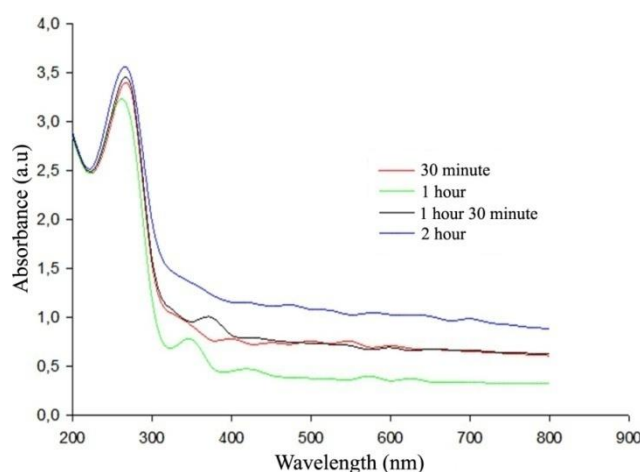
effect of holding time causes the size of the atomic radius to increase so that the density increases [27]. The rise and fall of the intensity depends on how to prevent the sample from being contaminated when doing research because the greater the temperature and the holding time, the lower the diffraction peak the higher the intensity with temperature and holding time.

**Table 1.** Relationship between intensity and diffraction angle.

$2\theta$	$h k l$	Intensity 30 minutes	Intensity 1 hours	Intensity 1 hours 30 minutes	Intensity 2 hours
22.76	1 0 0	67.9	173.1	184.5	190.0
32.19	1 1 0	1000	1000	1000	1000
38.43	1 1 1	242.5	273.8	316.5	361.4
47.73	2 0 0	366.5	373.4	427.1	386.4

### 3.2. The Results of the Absorbance Spectrum Measurement

The UV-Vis characterization of the BZT thin layer grown on the FTO substrate with the composition  $\text{Ba}(\text{Zr}_{0.5}\text{Ti}_{0.5})\text{O}_3$  shows the measurement results relating to the absorbance (representing the y axis) and the wavelength (representing the x axis). BZT thin films were grown using the sol-gel method with annealing temperature of 700 °C holding time 30 minutes, 1 hour, 1 hour 30 minutes and 2 hours to see the absorbance spectrum peaks at wavelengths. Figure 2 shows the UV-Vis results in the form of absorbance spectrum of BZT material at 700 °C holding time 30 minutes, 1 hour, 1 hour 30 minutes and 2 hours as shown below:



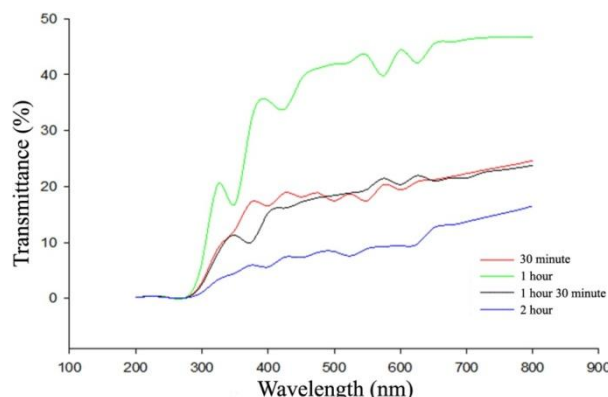
**Figure 2.** Optical absorbance spectrum of sample  $\text{Ba}(\text{Zr}_{0.5}\text{Ti}_{0.5})\text{O}_3$  holding time 30 minutes, 1 hour, 1 hour 30 minutes and 2 hours at 700 °C.

Figure 2 shows that in the UV-Vis spectroscopic measurement with the composition of the sample  $\text{Ba}(\text{Zr}_{0.5}\text{Ti}_{0.5})\text{O}_3$  holding time of 30 minutes, 1 hour, 1 hour 30 minutes and 2 hours at 700 °C, it turns out that it has different absorbance values at temperature. the same one. It can be seen in Figure 2 where the composition of  $\text{Ba}(\text{Zr}_{0.5}\text{Ti}_{0.5})\text{O}_3$  has a maximum absorbance value of 3.4244 arbitrary unit (a.u) with a holding time of 2 hours with a wavelength of 275 nm. At the same temperature with a different holding time, a different absorbance value occurs because the heated material becomes denser and homogeneous [18], so that the light transmitted to the heated material is not completely absorbed by the material but is scattered [27]. These data provide information that the higher the Zr composition [28,17] in the thin layer, the lower the resulting absorbance value and vice versa.

### 3.3. Measurement Results of the Transmittance Spectrum

The UV-Vis characterization of the BZT thin layer grown on the FTO substrate with the composition  $\text{Ba}(\text{Zr}_{0.5}\text{Ti}_{0.5})\text{O}_3$  shows the measurement results relating to the transmittance (representing the y-axis) and the wavelength (representing the x-axis). BZT thin films were grown using the sol-gel method with annealing temperature of 700 °C holding time of 30 minutes, 1 hour, 1

hour 30 minutes and 2 hours to see the peak of the transmittance spectrum at wavelengths. Figure 3 shows the UV-Vis results in the form of the transmittance spectrum of the BZT material at a temperature of 700 °C. Holding time 30 minutes, 1 hour, 1 hour 30 minutes and 2 hours as shown in figure 3.



**Figure 3.** Optical transmittance spectrum of sample  $\text{Ba}(\text{Zr}_{0.5}\text{Ti}_{0.5})\text{O}_3$  holding time 30 minutes, 1 hour, 1 hour 30 minutes and 2 hours at 700 °C.

Figure 3 explains that the curve can be seen the maximum and minimum transmittance value data with wavelengths, where the transmittance value can be calculated from the absorbance value obtained in Figure 2 using equation (1).

$$A = \log \frac{1}{T} = \log 1 - \log T \quad (1)$$

Sample  $\text{Ba}(\text{Zr}_{0.5}\text{Ti}_{0.5})\text{O}_3$  with a holding time of 30 minutes with a maximum transmittance value obtained  $\text{TM}_1$  20.328% and  $\text{TM}_2$  17.258%, minimum transmittance  $\text{Tm}_1$  17.418% and  $\text{Tm}_2$  16.477% with a wavelength of 1 ( $\lambda_1$ ) 575 nm wavelength 2 ( $\lambda_2$ ) 375 nm. Sample  $\text{Ba}(\text{Zr}_{0.5}\text{Ti}_{0.5})\text{O}_3$  with a holding time of 1 hour with a maximum transmittance value obtained  $\text{TM}_1$  44.477% and  $\text{TM}_2$  20.568%, minimum transmittance  $\text{Tm}_1$  39.811% and  $\text{Tm}_2$  16.753% with a wavelength of 1 ( $\lambda_1$ ) 600 nm wavelength 2 ( $\lambda_2$ ) 325 nm. Sample  $\text{Ba}(\text{Zr}_{0.5}\text{Ti}_{0.5})\text{O}_3$  with a holding time of 1 hour 30 minutes with a maximum transmittance value obtained  $\text{TM}_1$  21.953% and  $\text{TM}_2$  11.279%, minimum transmittance  $\text{Tm}_1$  20.342% and  $\text{Tm}_2$  10.007% with a wavelength of 1 ( $\lambda_1$ ) 625 nm wavelength 2 ( $\lambda_2$ ) 350 nm. Sample  $\text{Ba}(\text{Zr}_{0.5}\text{Ti}_{0.5})\text{O}_3$  with a holding time of 2 hours with a maximum transmittance value obtained  $\text{TM}_1$  10.859% and  $\text{TM}_2$  7.759%, minimum transmittance  $\text{Tm}_1$  9.725% and  $\text{Tm}_2$  7.163% with wavelength 1 ( $\lambda_1$ ) 675 nm wavelength 2 ( $\lambda_2$ ) 450 nm.

Figure 3 shows the transmittance relationship to the wavelength of the BZT thin layer at 700 °C with a holding time of 30 minutes, 1 hour, 1 hour 30 minutes and 2 hours. A thin layer of  $\text{Ba}(\text{Zr}_{0.5}\text{Ti}_{0.5})\text{O}_3$  at a holding time of 1 hour can be seen in Figure 3. The transmittance value is closely related to the quality of the resulting crystal. The higher the transmittance value [8], the better the crystal quality [17].

### 3.4. Bias Index Value and Thickness of BZT Material

Figure 3 explains that in the transmittance spectrum it can be seen that the data for the maximum transmittance value (TM) and minimum transmittance (Tm) with wavelengths, the calculation is obtained using equation 2 [29] as follows:

$$N = 2n_s \frac{T_M - T_m}{T_M T_m} + \frac{n_s^2 + 1}{2} \quad (2)$$

The value of refractive index (n) is obtained using equation 3 and the value of the thickness of the material (d) is obtained using equation 4 as shown in table 2 below:

$$n = \sqrt{N + \sqrt{N^2 - n_s^2}} \quad (3)$$

**Table 2.** Values of refractive index and thickness of thin films at 700 ° C.

Holding Time	$\lambda$ (nm)	$T_M$	$T_m$	n	d (m)
30 minutes	575	0.203	0.174	2.821	$1.293 \times 10^{-7}$
	375	0.173	0.165	2.103	
1 hours	600	0.444	0.398	2.082	$4.142 \times 10^{-7}$
	325	0.206	0.167	3.121	
1 jahours 30 minutes	625	0.219	0.203	2.237	$3.658 \times 10^{-7}$
	350	0.113	0.1	3.140	
2 hours	675	0.109	0.097	3.077	$2.190 \times 10^{-7}$
	450	0.078	0.072	3.075	

In Table 2 it can be explained that at a temperature of 700 °C, the values of  $\lambda$ ,  $T_M$ , and  $T_m$  are obtained in Figure 3. The value of n can be determined using equation (3). The value of d is determined using equation (4) as follows:

$$d = \frac{\lambda_1 \lambda_2}{2(\lambda_1 n_2 - \lambda_2 n_1)} \quad (4)$$

As the thickness of the layer increases, the grain diameter of the layers also increases. The increase in grain diameter [17] of the constituent of this thin film results in an increase in surface roughness, which in turn increases the scattering of photon waves on the surface of the layer [30].

The BZT thin layer grown by the Sol-gel method produced almost the same optical transmittance in the visible wavelength range. That is, at this thickness limit the thin layer does not produce a significant increase in photon scattering [18].

### 3.5. Absorption Coefficient Value and Energy Gap

The thin film absorption coefficient ( $\alpha$ ) is obtained using equation (5) as follows:

$$\alpha = -\frac{1}{a} \ln(T) \quad (5)$$

The method used to determine this energy bandgap is the Tauc Plot method, which is a method for determining the energy bandgap by extrapolating the linear region of the graph between photon energy ( $h\nu$ ) as the x-axis and the absorption coefficient of photons ( $\alpha h\nu$ )<sup>2</sup> as the y-axis. to cut the energy axis and the energy bandgap value is obtained. This energy bandgap graph was made using a sigma plot to determine the energy bandgap value in the BZT thin layer. The energy band gap (energy gap) is the energy required for electrons to break covalent bonds so that they can move from the valence band to the conduction band. This energy band gap determines a material including conductors, insulators and semiconductors. Figure 4 explains that ( $\alpha h\nu$ )<sup>2</sup> (representing the y-axis) to ( $h\nu$ ) (representing the x-axis).

Figure 4 (a) shows that on curve ( $\alpha h\nu$ )<sup>2</sup> to ( $h\nu$ ) thin layer Ba(Zr<sub>0.5</sub>Ti<sub>0.5</sub>)O<sub>3</sub> holding time 30 minutes for wavelength (200-800) nm after making a line with the Tauc method plot of the value ( $\alpha h\nu$ )<sup>2</sup> Until the line intersects with the x-axis, the energy gap value is obtained from the intersection of 3.95 eV. Figure 4 (b) shows that the curve ( $\alpha h\nu$ )<sup>2</sup> towards ( $h\nu$ ) thin layer Ba(Zr<sub>0.5</sub>Ti<sub>0.5</sub>)O<sub>3</sub> holding time 1 hour for wavelengths (200-800) nm after making a line with the Tauc method plot of the value ( $\alpha h\nu$ )<sup>2</sup> Until the line intersects with the x axis, the energy gap value is 3.98 eV from the intersection. Figure 4 (c) shows that the curve ( $\alpha h\nu$ )<sup>2</sup> towards ( $h\nu$ ) thin layer Ba(Zr<sub>0.5</sub>Ti<sub>0.5</sub>)O<sub>3</sub> holding time 1 hour 30 minutes for wavelength (200-800) nm after making a line with the Tauc method plot of the value ( $\alpha h\nu$ )<sup>2</sup> until the intersection of the line with the x-axis, from the intersection, the energy gap value is 3.94 eV. Figure 4 (d) shows that the curve ( $\alpha h\nu$ )<sup>2</sup> against ( $h\nu$ ) thin layer Ba(Zr<sub>0.5</sub>Ti<sub>0.5</sub>)O<sub>3</sub> holding time 2 hours for wavelengths (200-800) nm after making a line with the Tauc method plot of the value ( $\alpha h\nu$ )<sup>2</sup> Until the line intersects with the x axis, the energy gap value is obtained from the intersection of 3.92 eV.

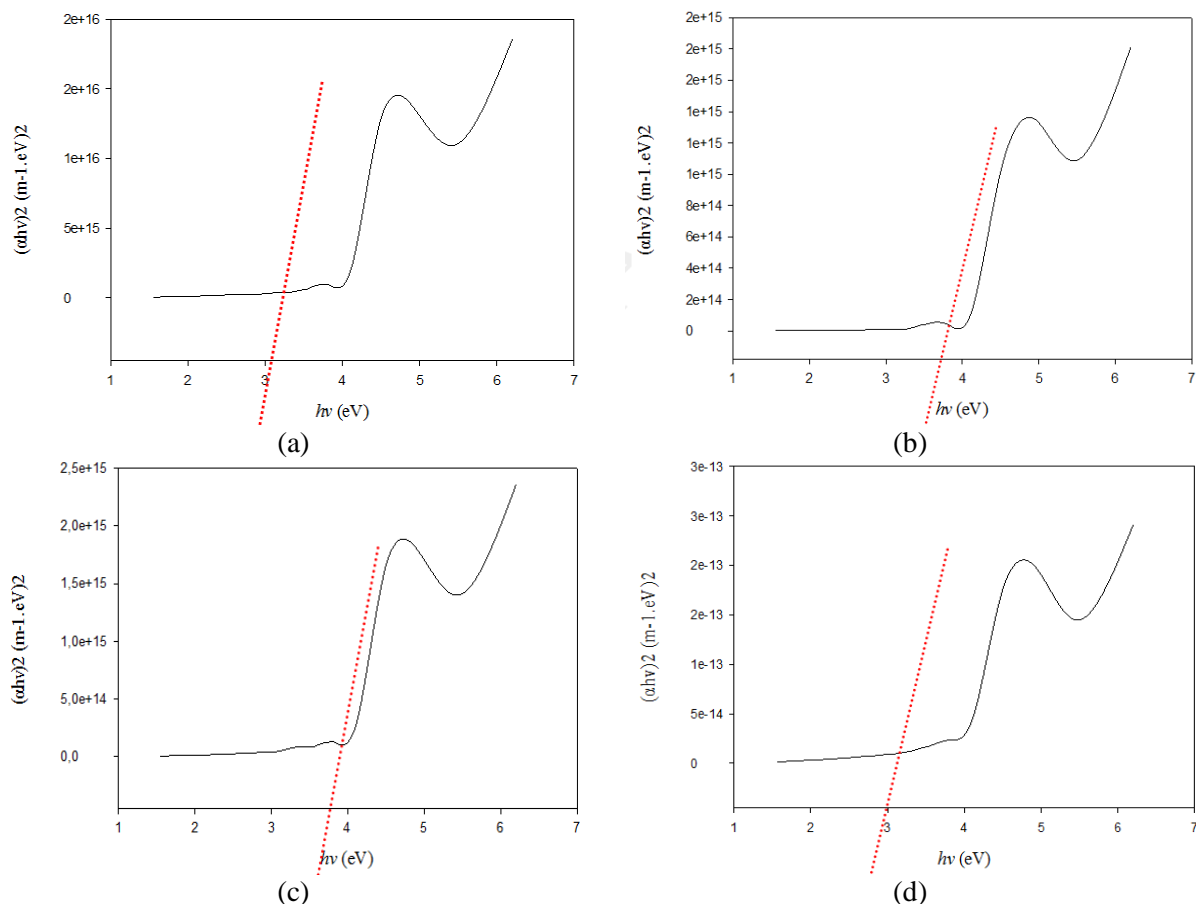


**Figure 4.** Curve  $(\alpha hv)^2$  against  $(hv)$  thin layer  $Ba(Zr_{0.5}Ti_{0.5})O_3$  holding time (a) 30 minutes; (b) 1 hour; (c) 1 hour 30 minutes; and (d) 2 hour at  $700\text{ }^\circ\text{C}$ .

**Table 3.** Value of energy gap at holding time temperature  $700\text{ }^\circ\text{C}$ .

<i> Holding Time</i>	<i> Energigap</i> (eV)
30 minutes	3,95
1 hours	3,98
1 hours 30 minutes	3,94
2 hours	3,92

Table 3 can be explained that in the thin layer  $Ba(Zr_{0.5}Ti_{0.5})O_3$  with different holding times using the Tauc plot method, namely extrapolating from the relationship graph  $(hv)$  as the x-axis abscissa and  $(\alpha hv)^2$  as the y-axis ordinate. to cut the energy axis so that the energy bandgap value is obtained. Cavalcante et al (2013) reported that the  $Ba(Zr_{0.25}Ti_{0.75})O_3$  thin layer of  $O_3$  was synthesized using the complex polymer method, the energy gap value was 3.78 eV at  $700\text{ }^\circ\text{C}$  for 2 hours under air pressure [18]. Lin et al (2012) reported that the thin layer  $Ba(Zr_xTi_x)O_{3-x}$  ( $Ba_{0.7}Ca_{0.3}$ )  $TiO_3$  used the sol-gel method by looking at the structure, dielectric, ferroelectric and optical properties [17]. At a temperature of  $700\text{ }^\circ\text{C}$  heated for 1 hour aims to get a crystalline structure with  $x = 0.5$  with a gap energy of 3.90 eV. Xin et al, (2011) reported that the structure and optical properties of thin layer  $Ba(Zr_xTi_x)O_3$  were grown on the MgO substrate with the Pulsed Laser Deposition method where  $x = 0$  to 0.4 with the largest energy gap of 3.92 eV [8]. Souza et al, (2016) explain the photoluminescence in  $Ba(Zr_xTi_x)O_3$  crystals using the hydrothermal method  $x = 5$  with an energy gap of 3.7 eV [28]. This is proven that in research conducted using various methods it has an energy gap as shown in Table 3, because the BZT material is an insulating dielectric material (conductor or semiconductor). So the energy gap generated in this study is a semiconductor material where the energy gap ranges from 1 eV to 4 eV.

#### 4. CONCLUSION

The preparation of a thin layer of BZT with the composition of  $\text{Ba}(\text{Zr}_{0.5}\text{Ti}_{0.5})\text{O}_3$  at annealing temperature of 700 °C has been successfully carried out. The variation of the holding time affects the size of the lattice crystal, the higher the annealing temperature or the holding time, the larger the lattice crystal size. The lattice parameter has a value of  $a = b \neq c$ , a value of  $a = b$  of 3.918 Å and a value of  $c$  of 4.102 Å. This shows that the crystal structure of BZT is tetragonal. Sample Ba (Zr0.5Ti0.5) O3 has a maximum absorbance value of 3,4244 arbitrary units (a.u) with a holding time of 2 hours with a wavelength of 275 nm. So the Zr composition affects the resulting absorbance, the lower the Zr composition in the thin layer, the higher the resulting absorbance and vice versa. Sample  $\text{Ba}(\text{Zr}_{0.5}\text{Ti}_{0.5})\text{O}_3$  with a holding time of 1 hour with a maximum transmittance value obtained  $\text{TM}_1$  44.477% and  $\text{TM}_2$  20.568%, minimum transmittance  $\text{Tm}_1$  39.811% and  $\text{Tm}_2$  16.753% with a wavelength of 1 ( $\lambda_1$ ) 600 nm wavelength 2 ( $\lambda_2$ ) 325 nm. The transmittance value is closely related to the quality of the resulting crystal. The higher the transmittance value obtained, the better the crystal quality. The energy band gap width obtained from the thin layer  $\text{Ba}(\text{Zr}_{0.5}\text{Ti}_{0.5})\text{O}_3$  with a holding time of 30 minutes, 1 hour, 1 hour 30 minutes and 2 hours at 700 °C respectively is 3.95 eV, 3.98 eV, 3.94 eV and 3.92 eV. Thus the energy band gap of the  $\text{Ba}(\text{Zr}_{0.5}\text{Ti}_{0.5})\text{O}_3$  thin layer includes the conductor material.

#### REFERENCES

- [1] Yan, Y., Ning, C., Jin, Z., Qin, H., Luo, W., & Liu, G. (2015). The dielectric properties and microstructure of  $\text{BaTiO}_3$  ceramics with  $\text{ZnO-Nb}_2\text{O}_5$  composite addition. *Journal of alloys and compounds*, 646, 748–752.
- [2] Jona, F., & Shirane, G., (1993). *Ferroelectric Crystal*–Paperback. Dover Pubns: Unabridged.
- [3] Wang, J., Zhang, X., Zhang, J., Li, H., & Li, Z. (2012). Dielectric and piezoelectric properties of  $(1-x)\text{Ba}_{0.7}\text{Sr}_{0.3}\text{TiO}_{3-x}\text{Ba}_{0.7}\text{Ca}_{0.3}\text{TiO}_3$  perovskites. *Journal of Physics and Chemistry of Solids*, 73(7), 957–960.
- [4] Aparna, M., Bhimasankaram, T., Suryanarayana, S. V., Prasad, G., & Kumar, G. S. (2001). Effect of lanthanum doping on electrical and electromechanical properties of  $\text{Ba}_{1-x}\text{La}_x\text{TiO}_3$ . *Bulletin of Materials Science*, 24(5), 497–504.
- [5] Majumder, S. B., Jain, M., Martinez, A., Katiyar, R. S., Van Keuls, F. W., & Miranda, F. A. (2001). Sol–gel derived grain oriented barium strontium titanate thin films for phase shifter applications. *Journal of Applied Physics*, 90(2), 896–903.
- [6] Arlt, G., Hennings, D., & De With, G. (1985). Dielectric properties of fine-grained barium titanate ceramics. *Journal of applied physics*, 58(4), 1619–1625.
- [7] Reinke, M., Kuzminykh, Y., Eltes, F., Abel, S., LaGrange, T., Neels, A., Fompeyrine, J., & Hoffmann, P. (2017). Low temperature epitaxial barium titanate thin film growth in high vacuum CVD. *Advanced Materials Interfaces*, 4(18), 1700116.
- [8] Xin, J. Z., Leung, C. W., & Chan, H. L. W. (2011). Composition dependence of structural and optical properties of  $\text{Ba}(\text{Zr}_x\text{Ti}_{1-x})\text{O}_3$  thin films grown MgO substrates by pulsed laser deposition. *Journal of Thin Solid Films*, 519, 6313–6318.
- [9] Bernardi, M., Giulianini, M., & Grossman, J. C. (2010). Self-assembly and its impact on interfacial charge transfer in carbon nanotube/P3HT solar cells. *ACS nano*, 4(11), 6599–6606.
- [10] Saputri, D. F., Hadiati, S., Ramelan, A. H., Iriani, Y., & Variani, V. (2013). Pengaruh doping stronsium pada lapisan tipis  $\text{BaZr}_{0.20}\text{Ti}_{0.8}\text{O}_3$ . *Jurnal Fisika dan Aplikasinya*, 9(2).
- [11] Tian, H. Y., Helen, L. W. C., Chung L. C., & Kwangsoo, N. (2002). The effects of composition gradients of  $\text{Ba}_x\text{Sr}_{1-x}\text{TiO}_3$  thin lapisans on their microstructures, dielectric and optical properties. *Journal Materials science and Engineering*, B103, 246–252.
- [12] Ozawa, T. C., & Kang, S. J. (2004). Balls&Sticks: easy-to-use structure visualization and animation program. *Journal of Applied Crystallography*, 37(4), 679–679.
- [13] Xiao, S. H., Jiang, W. F., Luo, K., Xia, J. H., & Zhang, L. (2011). Structure and ferroelectric properties of barium titanate films synthesized by sol–gel method. *Materials Chemistry and Physics*, 127(3), 420–425.

- [14] Ban, Z. G., & Alpay, S. P. (2002). Phase diagrams and dielectric response of epitaxial barium strontium titanate films: A theoretical analysis. *Journal of Applied Physics*, 91(11), 9288–9296.
- [15] Saputrina, T. T., Iwantono, I., Awitdrus, A., & Umar, A. A. (2020). Performances of Dye-Sensitized Solar Cell (DSSC) with Working Electrode of Aluminum-doped ZnO Nanorods. *Science, Technology & Communication Journal*, 1(1), 1–7.
- [16] Saroukhani, Z., Tahmasebi, N., Mahdavi, S. M., & Nemati, A. (2015). Effect of working pressure and annealing temperature on microstructure and surface chemical composition of barium strontium titanate films grown by pulsed laser deposition. *Bulletin of Materials Science*, 38(6), 1645–1650.
- [17] Lin, Y., Wu, G., Qin, N., & Bao, D. (2012). Structure, dielectric, ferroelectric, and optical properties of  $(1-x)\text{Ba}(\text{Zr}_{0.2}\text{Ti}_{0.8})\text{O}_{3-x}(\text{Ba}_{0.7}\text{Ca}_{0.3})\text{TiO}_3$  thin films prepared by sol-gel method. *Thin Solid Films*, 520(7), 2800–2804.
- [18] Cavalcante, L. S., Batista, N. C., Badapanda, T., Costa, M. G. S., Li, M. S., Avansi, W., Mastelaro, V. R., Longgo, E., Espinosa, J. W. W., & Gurgel, M. F. C. (2013). Local electronic struktur, optical bandgap and photoluminescence (PL) Properties of  $\text{Ba}(\text{Zr}_{0.75}\text{Ti}_{0.25})\text{O}_3$  powder. *Journal of materials Science in Semiconductor Processing*, 16, 1035–1045.
- [19] Challali, F., Besland, M. P., Benzeggouta, D., Borderon, C., Hugon, M. C., Salimy, S., Saubat, J.C., Charpentier, A., Averty, D., Goullet, A., & Landesman, J. P. (2010). Investigation of BST thin films deposited by RF magnetron sputtering in pure Argon. *Thin Solid Films*, 518(16), 4619–4622.
- [20] Resendiz-Munoz, J., Fernandez-Munoz, J. L., Farias-Mancilla, J. R., Melendez-Lira, M., Medel-Juarez, J. J., & Zelaya-Angel, O. (2018).  $\text{Ba}_x\text{Sr}_{1-x}\text{TiO}_3$  nanocrystalline thin films deposition grounded In RF magnetron co-sputtering. *Digest Journal Of Nanomaterials And Biostructures*, 13(3), 751–758.
- [21] Jian, G., Jiao, Y., Meng, Q., Cao, Y., Zhou, Z., Moon, K. S., & Wong, C. P. (2020). Hydrothermal synthesis of  $\text{BaTiO}_3$  nanowires for high energy density nanocomposite capacitors. *Journal of Materials Science*, 55(16), 6903–6914.
- [22] Xie, H., Biswas, M., Fan, L., Li, Y., & Su, P. C. (2017). Rapid thermal processing of chemical-solution-deposited yttrium-doped barium zirconate thin films. *Surface and Coatings Technology*, 320, 213–216.
- [23] Hemedi, O. M., Eid, M. E. A., Sharshar, T., Ellabany, H. M., & Henaish, A. M. A. (2021). Synthesis of nanometer-sized  $\text{PbZr}_x\text{Ti}_{1-x}\text{O}_3$  for gamma-ray attenuation. *Journal of Physics and Chemistry of Solids*, 148, 109688.
- [24] Pontes, F. M., Longo, E., Leite, E. R., & Varela, J. A. (2001). Study of the dielectric and ferroelectric properties of chemically processed  $\text{Ba}_x\text{Sr}_{1-x}\text{TiO}_3$  thin films. *Journal of Thin Solid Films*, 386, 91–98.
- [25] Iwan, S., Zhao, J. L., Tan, S. T., & Sun, X. W. (2018). Enhancement of UV photoluminescence in ZnO tubes grown by metal organic chemical vapour deposition (MOCVD). *Vacuum*, 155, 408–411.
- [26] Instan, A. A., Pavunny, S. P., Bhattarai, M. K., & Katiyar, R. S. (2017). Ultrahigh capacitive energy storage in highly oriented  $\text{Ba}(\text{Zr}_x\text{Ti}_{1-x})\text{O}_3$  thin films prepared by pulsed laser deposition. *Applied Physics Letters*, 111(14), 142903.
- [27] Liman, J., Harsono, B., Rohman, T. T., Trimukti, U., Khalid, M., & Roharti, E. (2015). Uji Sifat Optik Film Tipis  $\text{Ba}_{0.55}\text{Sr}_{0.45}\text{TiO}_3$  di Atas Substrat Corning Glass 7059. *Jurnal Fisika Indonesia*, 19(56).
- [28] Souza, A. E., Sasaki, G. S., Camacho, S. A., Teixeira, S. R., Li, M. S., & Longo, E. (2016). Defects or charge transfer: Different possibilities to explain the photoluminescence in crystalline  $\text{Ba}(\text{Zr}_x\text{Ti}_{1-x})\text{O}_3$ . *Journal of Luminescence*, 179, 132–138.
- [29] Mulato, M., Chambouleyron, I., Birgin, E. G., & Martinez, J. M. (2000). Determination of thickness and optical constants of amorphous silicon films from transmittance data. *Applied Physics Letters*, 77(14), 2133–2135.
- [30] Yu, J., Zhao, X., & Zhao, Q. (2000). Effect of surface structure on photocatalytic activity of  $\text{TiO}_2$  thin films prepared by sol-gel method. *Thin solid films*, 379(1-2), 7–14.